Supporting Information

A-Site High-Entropy Engineering Enables a Cobalt-Free Perovskite Air Electrode with Exceptional Activity and Durability for Reversible Solid Oxide Cells

Chenshuo Yuan[a], Huanbin Zhang[a], Hui Ye[a], Pengkai Shan[a], Bo Yin[b], Sheng Cui [a], Yifeng Zheng[a, *]
[a]College of Materials Science and Engineering, Nanjing Tech University, No. 30 Puzhu Road(S), Nanjing, 211816, Jiangsu, China
[b]Morgan Thermal Ceramics (Shanghai) Co., Ltd. 18 Kang An Road, Kang Qiao Industrial Zone, Pudong, Shanghai, 201315, China

Supporting figures

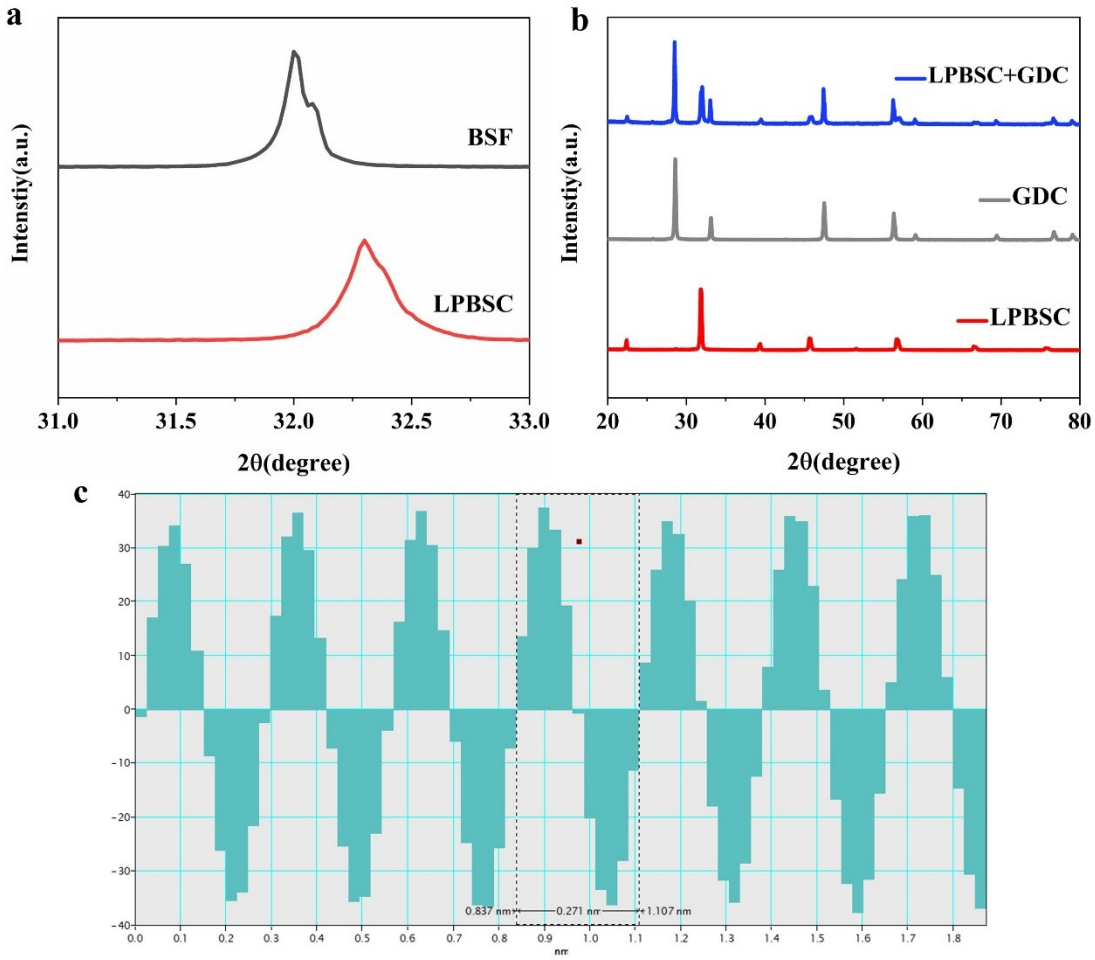

* Corresponding author
E-mail addresses: zhengyifeng@njtech.edu.cn (Y. Zheng)

Fig. S1. (a)Magnified section of XRD patterns, 2θ = 31.5−32°; (b) XRD patterns of LPBSC/GDC sintered at 1100 °C for 5 h; (c)The inverse fast fourier transform (IFFT) image of LPBSC.

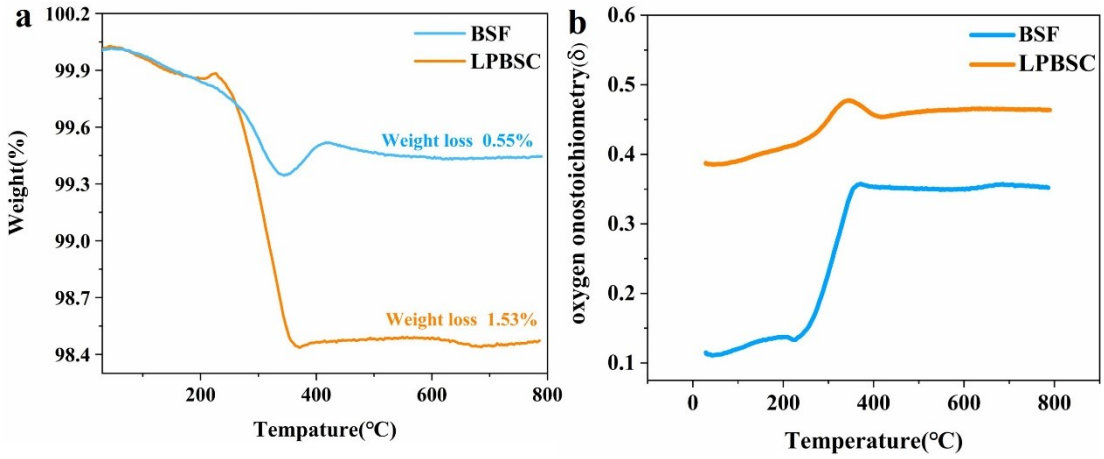

Fig. S2. (a) TGA curves of BSF and LPBSC; (b) Oxygen non-stoichiometry (δ) of BSF and LPBSC between 30-800 °C.

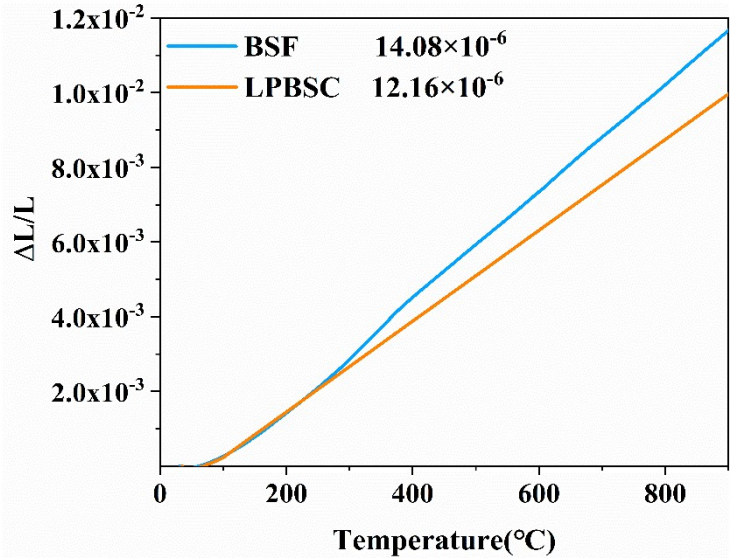

Fig. S3. Thermal expansion curves of BSF and LPBSC.

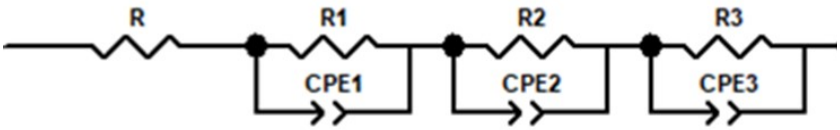

Fig. S4. Equivalent circuit of the BSF and LPBSC half-cell process.

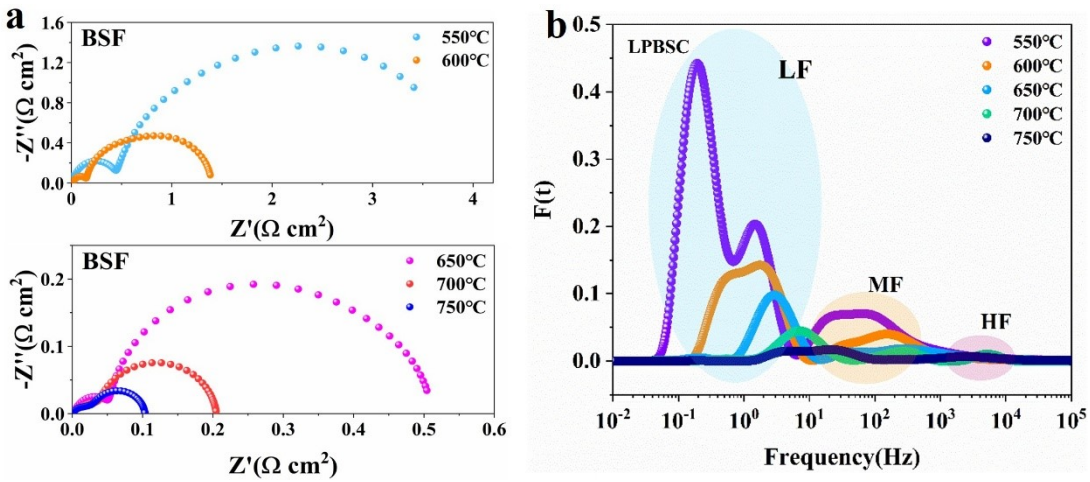

Fig. S5. (a) EIS curves of BSF air electrodes at 550-750 ℃; (b) DRT analysis of LPBSC at different temperatures.

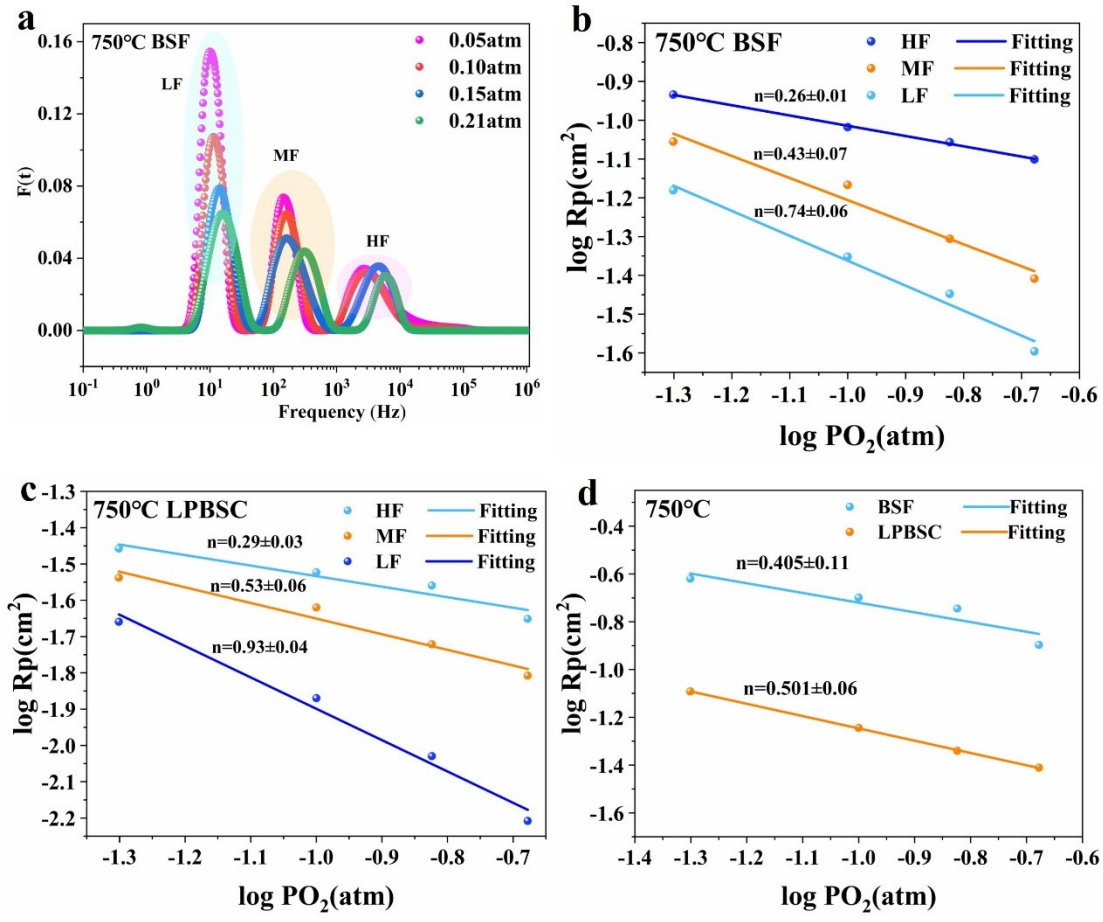

Fig. S6. (a) schematic illustration of the oxygen reduction reaction; The rate-limiting step of R_{HF}, R_{MF}, and R_{LF} in (b) BSF; (c) LPBSC;(d) Rp value of BSF and LPBSC under different PO_2 at 750 ℃;

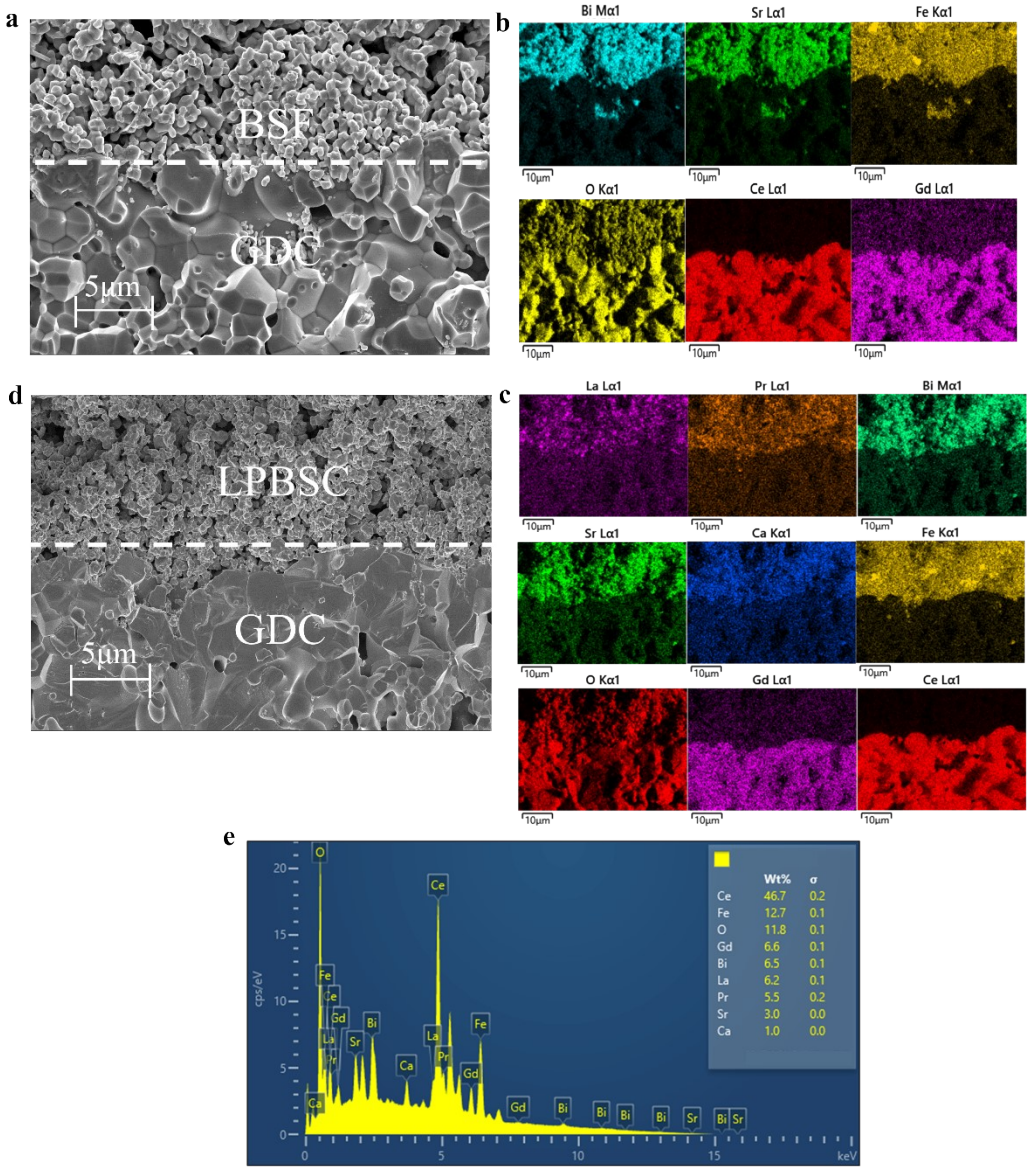

Fig. S7. (a)The cross-section SEM of the BSF half-cell After the stability test; (b) Cross-sectional EDX mapping of Fig. S7(a); (c) The cross-section SEM of the LPBSC half-cell After the stability test; (d) Cross-sectional EDX mapping of Fig. S7(c); (e) The simulated plots of the LPBSC half-cell atomic ratio.

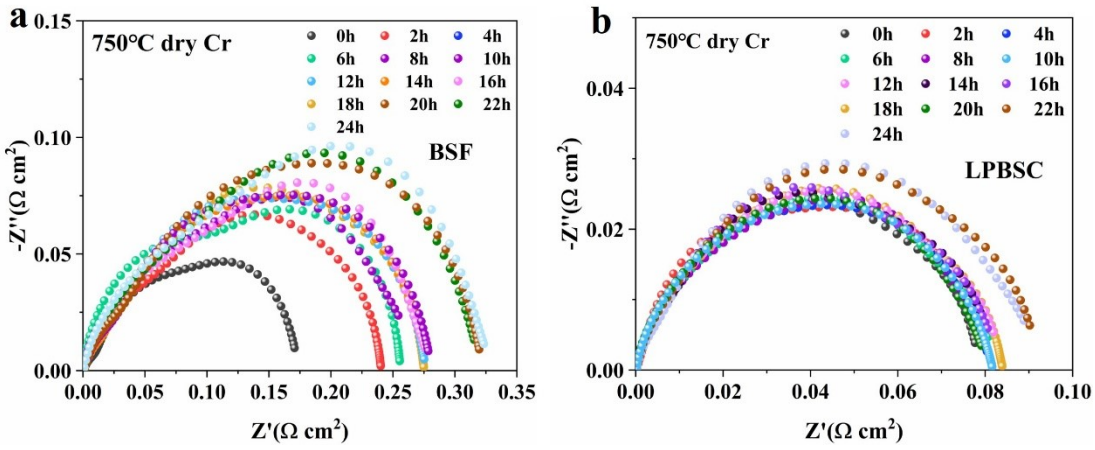

Fig. S8. EIS spectra of symmetric cells at 750 °C with Cr contamination in dry air for 24h (a) BSF; (b) LPBSC.

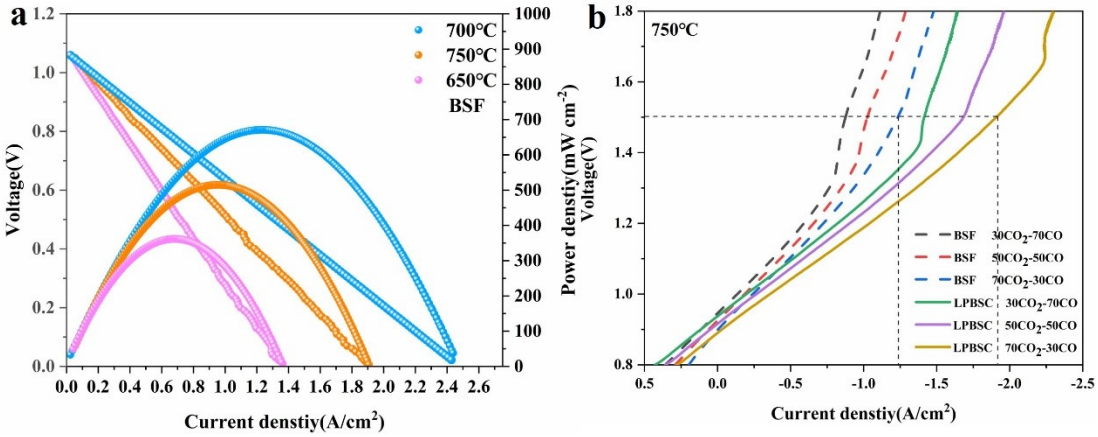

Fig. S9. (a) I–V–P curves of the single cell with BSF electrodes in dry H_2 at different temperatures; (b) I–V curves of the single cell with BSF and LPBSC electrodes for CO_2 electrolysis in different atmospheres.

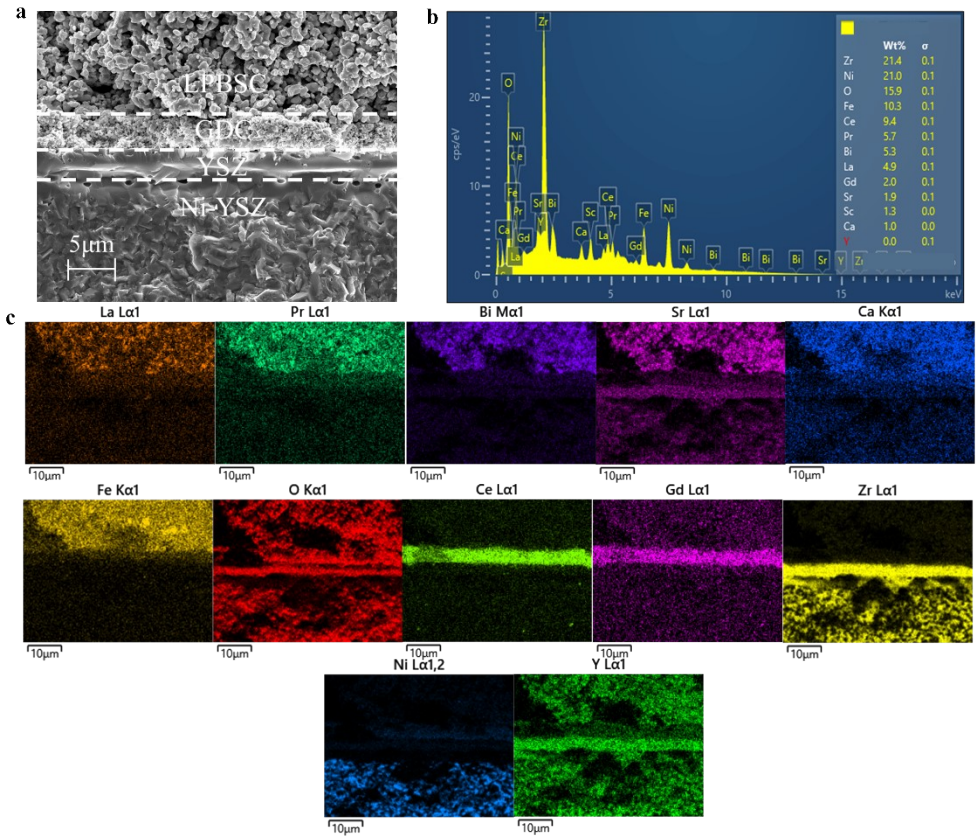

Fig. S10. (a)Cross-sectional SEM of LPBSC full-cell after stability test; (b) The simulated plots of the LPBSC full-cell atomic ratio ;(c) Cross-sectional EDX mapping of Fig. S9(a).

Table S1

The electrical conductivities of BSF and LPBSC at different temperatures

Temperature(℃)	LPBSC (S cm^{-1})	Temperature(℃)	BSF (S cm^{-1})
300	9.022	300	0.32081
330	11.69118	350	0.53709
360	14.5676	400	0.79384
390	17.23577	450	0.98171
420	19.97874	500	1.18518
450	22.31668	550	1.36316
480	24.48454	600	1.5017
510	25.99249	650	1.57532
540	25.99249	700	1.56075
570	25.22595	750	1.59644
600	24.24394	800	1.67159
630	23.14081		
660	22.23435		
690	20.95935		
720	19.90525		
750	18.7651		
780	17.42837		
800	16.91914		

Table S2

The $R_{total,}$ R_{ohm}, and ASR values of BSF and LPBSC air electrodes at 750°C.

Samples	R_{total} (Ω cm^2)	R_{ohm} (Ω cm^2)	ASR (Ω cm^2)
BSF	1.452	1.061	0.1955
LPBSC	1.088	0.967	0.0605

Table S3

Polarization Resistance (Rp) of Different Perovskite Air Electrode Materials at 650–750 °C

T/°C		650°C	700°C	750°C
Rp/Ω cm^2	$La_{0.2}Pr_{0.2}Sm_{0.2}Nd_{0.2}Sr_{0.2}FeO_{3-\delta}$	0.35	0.25	0.15
	$La_{0.6}Sr_{0.4}Co_{0.2}Fe_{0.8}O_{3-\delta}$	1.026	0.331	0.112
	$Ba_{0.2}Sr_{0.2}La_{0.2}Pr_{0.2}Sm_{0.2}FeO_{3-\delta}$	1.034	0.374	0.154
	$Ba_{0.35}Sr_{0.35}La_{0.1}Pr_{0.1}Sm_{0.1}FeO_{3-\delta}$	0.506	0.199	0.090
	$Sr_{0.2}Ba_{0.2}Bi_{0.2}La_{0.2}Pr_{0.2}FeO_{3-\delta}$	1.1	0.42	0.21
	$La_{0.2}Pr_{0.2}Ba_{0.2}Sr_{0.2}Ca_{0.2}FeO_{3-\delta}$	0.28	0.13	0.063
	BSF	0.5	0.2	0.1
	LPBSC	0.21	0.103	0.059